CHAPTER THREE

COMPUTER SIMULATION STUDY of THE GAY - BERNE MESOGEN

3.1 Introduction

Review of Liquid Crystal Simulations

Although computer simulation techniques have advanced considerably since their introduction in the early 1950's, the studies on liquid crystals have been conducted only recently, because of the molecular complexity of most mesogens which require a large number of interaction sites to construct a realistic potential. Furthermore, larger system size is needed to investigate weak mesophase transitions and long range order. Accordingly the earlier simulation have not attempted to simulate the actual liquid crystal molecule but instead a much simplified model which has the essential features dictating the phase behaviour. For instance, although the Lebwohl-Lasher model is unrealistic in that the particles possess no translational degrees of freedom, it appears to exhibit the orientation order-disorder transition [50] depicting nematic undergoing into the isotropic phase. Hard core models have been particularly successful in predicting a range of mesophases [51] and provide valuable insights into the role of excluded volume effects. "Soft" potentials, such as the Gaussian overlap model proposed by Berne and Perchukas [52], allow us to examine the influence of the attractive as well as the repulsive components of the intermolecular potential. In this section we review some of the models used in the computer simulation studies of liquid crystals.

(a) The Lebwohl -Lasher Model

In 1972, Lebwohl and Lasher [53] constructed a model for liquid crystal consisting of uniaxial rod-like particles. The uniaxial particles are placed on the sites of a simple cubic lattice, interacting through a nearest neighbour anisotropic pair potential of the form,

$$U_{ij} = -\epsilon_{ij} P_2(\cos\beta_{ij}), \qquad (3.1)$$

where ϵ_{ij} is a positive constant ϵ for nearest neighbour i and j but zero for other pairs; β_{ij} is the angle between the two particles. Being the earliest, the Lebwohl- Lasher model is one of the most studied liquid crystal systems by many different research groups and for different purposes including to test the Maier Saupe molecular field theory [54]. A number of simulations have been conducted using the lattice size system, typicallly, 10*10*10 [55] and 20*20*20 [53,56,57]. The nematic- isotropic transition temperatures were reported to exist between 1.119 and 1.127 for the larger system. In order to reduce the uncertainty in the location of the transition, Fabbri and Zannoni have performed simulations with a 30*30*30 lattice [54] and found the transition temperature to be 1.1232+ 0.0006.

(b) Hard Core Models

The relative success of the Maier-Saupe theory suggests that anisotropic attractive forces may be important in the formation of liquid crystal phases. However, it is generally accepted that the structure of a simple dense liquid is largely determined

by short range repulsive forces [58]. Alder and Wainwright showed in 1957 that the freezing of atomic liquid could be understood in term of the fluid-solid transition of hard spheres [59]. Of course, the situation for more "complex" phases such as liquid crystals, may be quite different. The relative importance of attractive or repulsive forces in determining liquid-crystaline behaviour is the subject of considerable discussion.

The short range component of the potential can be conveniently modelled by hard potentials which are defined with respect to some minimum contact distance σ such that,

$$U(r)= 0;\ for\ r > \sigma,$$
$$U(r)= \infty;\ for\ r \leq \sigma \qquad (3.2)$$

For molecules forming liquid crystal phases σ will thus be orientation dependent. The first prediction of the importance of short range forces in orientational transition was made by Onsager who showed, that at a sufficiently high density, a system of long, rod-like molecules would spontaneously form a nematic phases [60]. These early theoretical investigation were followed by computer simulations of hard ellipses [61] and spherocylinders by Vieillard-Baron [62]. In recent years, Frenkel and coworkers [51,63,64,65] have reported simulations involving an extensive diversity of hard core models. In thier computer simulations it is shown that hard prolate and oblate ellipsoids of revolution and spherocylinders can form nematic and, in some cases, smectic and columnar phases depending on the molecular size and shape. The molecular shape, as well as molecular size, is found to be relevent in stabilizing liquid crystal phases. It is

useful to examine the hard ellipsoids of revolution because they may resemble those due to the Gay-Berne potential, which has an essentially ellipsoidal repulsive component.

c) The Gay-Berne potential

A model involving both approaches, i.e. one which explicitly the anisotropic short range repulsive as well as the anisotropic long range attractive interactions, would be closer to real mesogenic systems. In this direction, Berne and Pechukas proposed a single-site potential based on the Gaussian overlap model [52]. In this model each molecule is represented by an ellipsoidal Gaussian distribution of forces centres. The interaction energy between two molecules is calculated by evaluating the overlap integral of the two Gaussians. The value of this integral involves quantities that can be identified, where the single -side potential in which the well depth, ϵ , and the size parameter, σ, depend on the orientations of the two particles , $\hat{\mathbf{u}}_1$, $\hat{\mathbf{u}}_2$, and of the intermolecular vector, **r**. The particular form chosen for the Gay -Berne potential is a shifted Lennard -Jones 12 - 6 potential,

$$U(\hat{\boldsymbol{u}}_1,\hat{\boldsymbol{u}}_2,\boldsymbol{r}) = 4\epsilon(\hat{\boldsymbol{u}}_1,\hat{\boldsymbol{u}}_2,\boldsymbol{r})\left[\frac{\sigma_o}{(r-\sigma(\hat{\boldsymbol{u}}_1,\hat{\boldsymbol{u}}_2,\boldsymbol{r})+\sigma_o}\right]^{12} - \left[\frac{\sigma_o}{(r-\sigma(\hat{\boldsymbol{u}}_1,\hat{\boldsymbol{u}}_2,\boldsymbol{r})+\sigma_o}\right]^{6}, \qquad (3.3)$$

where $\hat{\boldsymbol{u}}_1$ and $\hat{\boldsymbol{u}}_2$ are unit vectors giving the orientation of the symmetry axes for the two particles and the orientation of the intermolecular vector is denoted by $\boldsymbol{r}$ (see Fig. 3.1(a)). The parameters in the potential are orientation dependent where $\epsilon(\hat{\boldsymbol{u}}_1,\hat{\boldsymbol{u}}_2,\boldsymbol{r})$ is the well depth and $\sigma(\hat{\boldsymbol{u}}_1,\hat{\boldsymbol{u}}_2,\boldsymbol{r})$ is the intermolecular separation at which the attractive

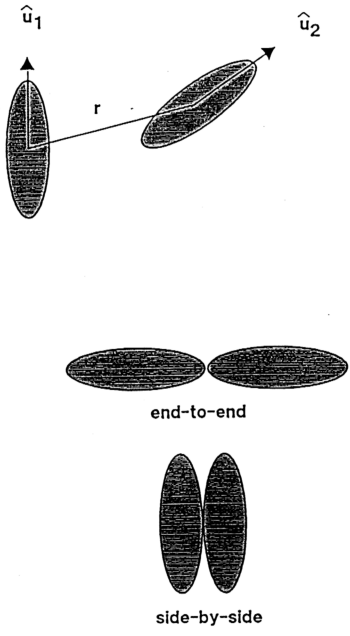

Fig. 3.1 (a) Two Berne-Pechukas particles with orientations $\hat{u}_1$ and $\hat{u}_2$.
(b) The end-to-end and side-by-side configurations.

and repulsive terms cancel. The functional dependence of this distance is, as in the Berne-Pechukas-Kushick potential,

$$\sigma(\hat{u}_1,\hat{u}_2,r) = \sigma_0 \left[(1-\frac{\chi}{2})\left[\frac{(\hat{u}_1.r + \hat{u}_2.r)^2}{(1+\chi(\hat{u}_1.\hat{u}_2)}\right] + \left[\frac{(\hat{u}_1.r - \hat{u}_2.r)^2}{(1-\chi(\hat{u}_1.\hat{u}_2)}\right], \qquad (3.4)$$

where σ_0 is a constant. The shape anisotropiy parameter, χ, is

$$\chi = \left[\left(\frac{\sigma_e}{\sigma_s}\right)^2 - 1\right] / \left[\left(\frac{\sigma_e}{\sigma_s}\right)^2 + 1\right], \qquad (3.5)$$

where σ_e is the contact separation when the molecule are end-to-end and σ_s that when they are side-by-side (see Figure 3.1(b)). In other words σ_e and σ_s are essentially the length and breath of the particle; χ vanishes for spherical particles and is one for infinitely long rods and minus one for infinitely thin disks.

The depth of the well is writen as,

$$\epsilon(\hat{u}_1,\hat{u}_2,r) = [\epsilon(\hat{u}_1,\hat{u}_2)]^{\nu}[\epsilon'(\hat{u}_1,\hat{u}_2,r)]^{\mu}, \qquad (3.6)$$

where,

$$\epsilon(\hat{u}_1,\hat{u}_2) = \frac{\epsilon_o}{[1-\chi^2(\hat{u}_1,\hat{u}_2)^2]^{1/2}}, \qquad (3.7)$$

as in the original Berne-Pechukas-Kushick potential[52].

The second part has a form similar to that of $\sigma(\hat{u}_1,\hat{u}_2,r)$, namely

$$\epsilon'(\hat{u}_1,\hat{u}_2,r) = (1 - \frac{\chi'}{2})[\frac{(\hat{u}_1.r + \hat{u}_2.r)^2}{(1 - \chi'(\hat{u}_1.\hat{u}_2)}] + [\frac{(\hat{u}_1.r - \hat{u}_2.r)^2}{(1 - \chi'(\hat{u}_1.\hat{u}_2)}], \qquad (3.8)$$

where the parameter χ' is related to the anisotropy in the well depth via

$$\chi' = [(\frac{\epsilon_e}{\epsilon_s})^{\frac{1}{\mu}} - 1] / [(\frac{\epsilon_e}{\epsilon_s})^{\frac{1}{\mu}} + 1], \qquad (3.9)$$

where ϵ_e and ϵ_s are well depths for the end-to-end and side-by-side configurations. The values of μ and ν were obtained from the optimum fit to a line of four equidistant Lennard-Jones centres with a separation of 2σ between the first and fourth sites (see Fig. 3.2). In our simulation we have chosen that an axial ratio of σ_e/σ_s were set to 3.0 and the well depth ratio of ϵ_s/ϵ_e were set to 5, ν and μ were set to 1 and 2 respectively. The choice of parameter in this simulation are consistent with those used in the previous simulation [66,67,68]. It should be noted that, this intermolecular potential depends on four arbitrary parameters σ_e/σ_s, ϵ_s/ϵ_e, ν and μ which means that there is no unique Gay-Berne model mesogen but a whole variety just as there are many molecular structures capable of yeilding liquid-crystal phases. For instance, to parameterise the potential typical disc-like molecules e.g triphenylene σ_e/σ_s, was found to be about 0.345 while ϵ_e/ϵ_s was determined to be approximately 9.0 [69]. Luckhurst et al.[70] employed the values ν and μ to be taken as 2.0 and 1.0 respectively in thier

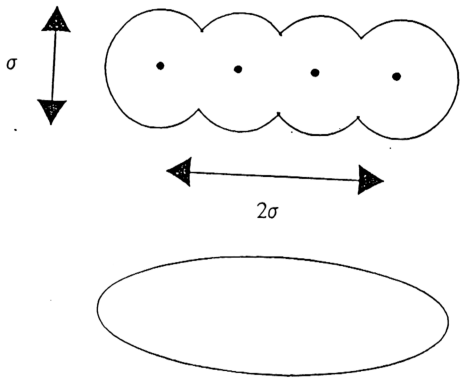

Fig. 3.2 Comparison of a Gay-Berne particle with a length: breadth ratio of 3:1 and a line of four Lennard- Jones centre.

Gay-Berne simulations where the parameter was chosen in order to enhance the formation of discotic nematic mesophases.

(d) Realistic Atom- atom Models

Rapid advances in computer technology has enable some workers to simulate realistic atom-atom potential for liquid crystal system, such as Komolkin et al. have reported Monte Carlo simulation of 64 4-ethoxybenzylidene-4' -n-butyaniline (EBBA) molecules [71]. In atom -atom potential, thier results, appear to suggest the formation of a nematic phase with features similar to those observed experimentally for EBBA. Similar studies have also been performed for systems of CCH5 molecules (trans-4-(trans-4-n-pentyl-cyclohexyl)cyclohexylcarbonitrile) [72] and for 5CB (4-n-pentyl-4'-cyanobiphenyl) [73]. The major limitation with these investigations is that only a small number of particles can be used. It is also somewhat limited by the length of the runs and the size of the system and therefore are not intended to provide a through account of the phase behaviour of such compounds.

3.2 The Simulation Details

The aim of this work is to study the cooling behaviour of the Gay-Berne model system at constant pressure, using Monte -Carlo (MC) simulation technique. Studies on this system have been conducted previously [67,68,74] but the cooling behaviour was not investigated. Since this is a simulation of an isothermal-isobaric ensemble, a direct

comparison with the real measurement can be made. Real thermotropic liquid crystals compounds examples like 4,4'-dimethoxyazoxybenzene, terphenyl, alkane hydrocarbon and paraazoxyanisole (PAA) were used in this study for comparison purpose.

Parameterisation

The Gay-Berne potential as described in section 3c was parameterised in the following manner. The length- to-breath, σ_e / σ_s, was set equal to 3 and the ratio for the well depths ϵ_s / ϵ_e was given the value of 5 . We also used the exponents ν and μ as 1 and 2 respectively. These are the values orginally proposed by Gay and Berne [75]. The scaled temperature is defined T* as,

$$T^* = k_B T / \epsilon_0, \qquad (3.10)$$

where k_B is the Boltzmann constant and ϵ_0 is the strength parameter, other scaled quantities are defined as the scaled volume, V*,

$$V^* = V / N\sigma_0^3, \qquad (3.11)$$

and the scaled pressure, p*,

$$p^* = p / \epsilon_0 \sigma_0^{-3}, \qquad (3.12)$$

where for prolate ellipsoids the contact parameter, σ_0 , which is used to scale quantities in the simulation is equal to σ_s. The number of particles, N, studied in this isothermal-isobaric Monte-Carlo simulation was 500 . The box dimensions were scaled with respect

to σ_0 but for computational convenience the components of the centre of mass coordinates were scaled with lengths of the respective side of the simulation box. The 500 particles were placed in an orthogonal simulation box which was surrounded by the usual periodic images. The spherical cut-off for the potential, r_c^* was set so that,

$$r_c^{*2} = \frac{V^{*2/3}}{4}, \qquad (3.13)$$

which correspond to a value in the range 3-4 or the interaction with 3-4 shells of neighbouring particles within a layer but only with molecules in the adjacent layers. The simulations were conducted at the scaled pressure , p* of 1.0, This value was chosen because it is sufficiently low to stabilise the smectic phases; indeed at higher pressure the nematic phases is stable. For a typical mesogen eg. 4,4'-dimethoxyazoxybenzene, where σ is about 4.5×10^{-10} m and the nematic and isotropic transition temperature is 408K at atmospheric pressure ($1.01 \times 10^{5} Nm^{-2}$), this scaled presure where $p^* = 1$ is correspond to presure of $5.83 \times 10^{7} Nm^{-2}$ which is 575 atm.

We implemented the Metropolis Monte- Carlo technique over the simulation where the average of any property is an NpT system is defined as,

$$<A>=Z^{-1}\int dV.ds.\exp(-\beta pV)V^N\exp(-\beta U) \qquad (3.14)$$

where Z is the partion function, ds is the integration over the particles scaled coordinates, dV = dx.dy.dz intergration are the volume of the box. The constant pressure Monte -Carlo method is similar to the convention constant volume Monte -

Carlo but the fact that a random volume changes is a legitimate Monte - Carlo move. Whether or not such a move is accepted depends on the change in the value of the weighting function ω:

$$\omega = \exp(-\beta p V)\, V^{N} \exp(-\beta U), \tag{3.15}$$

If V is changed by an amount ΔV, then $r = \omega_{New}/\omega_{Old}$ is given by

$$r = \exp[-\beta(\Delta V + p\Delta V - NkT\ln((V+\Delta V))/V))], \tag{3.16}$$

If $r \geq 1$ the move is accepted; if $0 < r < 1$, r is compared with a random number $0 < x < 1$, the move is accepted if $x \leq r$. It is important that the random moves ΔV be chosen such that any Markov chain in V is reversible. Performing the reversible random walk in ln V rather than in V is more convienient [76]. As a consequence the weighting function changes to ω';

$$\omega' = \exp(-\beta p V)\, V^{N+1} \exp(-\beta U). \tag{3.17}$$

The simulation contained two types of move namely isobaric and canonical move. In the canonical move where there is a change in the positions of the particles. For canonical move a particle was selected at random and random changes were made to both its position and orientation. The orientation of the particle was changed using the Barker-Watts procedure in which the particle is rotated by a random amount about a laboratory axis selected at random [77]. The maximum displacements were selected on a trial and error basis to achieve an acceptance ratio of 1/2, which was mention in earlier

in chapter 2. In the isobaric move where there is a change to the dimension of the simulation box hence the box volume orthogonality remained. These was achieved by making random alterations to the three components of the centre-of-mass coordinates subject to the same maximum displacement The isobaric move, can be acheive in three ways. First method random changes were made to the logarithms of all three box dimensions. For a second method the logarithm of two box lengths were also changed randomly (actually changing the area of the box) keeping one side constant. Thirdly changing one of the logarithm of its lengths at a time randomly while keeping the both lengths constant. Sampling the logarithm of one box length at a time to change the volume was proven to be more computationally efficient because the domain of the random walk in log V coincides with the range of acceptable (positive) values of V. Moreover the average stepsize in log V is much less density-dependent than the stepsize in V [76]. Therefore we have chosen this method to randomly change the log V of our box.

Starting Configuration

The starting configurations for the simulations were prepared in the following way. A configuration taken from heating sequence of the isotropic phase which had been prepared as part of Monte - Carlo study [74] with scaled pressure, p^* of 1 and a scaled temperature, T^* of 0.80. This was then studied at P^* of 1.0, and T^* of 0.70 for 48000000 cycles, where each cycle is N +2 attempted moves. The system was then cooled further at another six temperatures where (T^* = 0.65, 0.60, 0.55, 0.50, 0.45,

0.40) the scaled temperature of the sample was then lowered to 0.65 from T* of 0.70, at this stage 48000000 cycle was generated in order to equilibrate the system with initial configurations for the simulation are being taken from the production stage of the preceeding temperature. Next scaled temperature, T* of 0.60 was equilibrated for 149000000 MC cycles. This process was repeated for the remaining scaled temperatures (where T* of 0.55, 0.50, 0.45 and 0.40). Each of the final configurations generated in this way for all of the temperatures were then equilibrated further for the production stage.

3.3 Results and Discussion

3.3.1 Phase Identification and Artefact

In this simulation, various phases observed were identified using a qualitative approach of graphic visualization. We have developed a C language programme called KRISTAL using a Graphic-Library. The visualization allows us to take a configuration from the simulation and examine different features of molecular organization within the system. Images photographed from the screen of an RISC 350/6000 are shown in Fig. 3.3 for the simulations at scaled temperatures of approximately a) 0.70, b) 0.65, c) 0.60 and d) 0.55. In the images the 500 molecules are represent as lines whose length is that of 3:1 ratio of the Gay-Berne mesogen.

The configuration at the highest scaled temperature which is at T* of 0.70, see Fig. 3.3 (a) has the lowest order as is evident from the essentially random arrangement

a) V* = 3.82

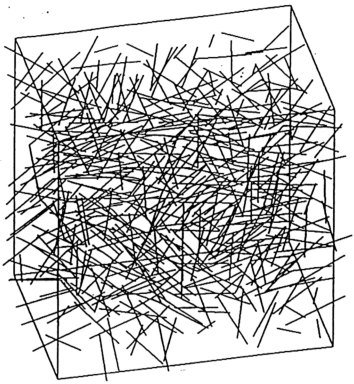

b) V* = 3.72

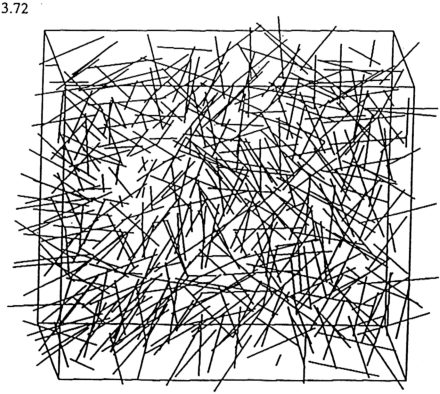

Fig. 3.3 Snapshot of the final molecular configurations for reduced temperature on cooling cycles of the NpT simulation consisting of 500 molecules:

a) T* of 0.70 (isotropic)
b) T* of 0.65 (isotropic)
c) T* of 0.60 (isotropic)
d) T* of 0.55 (smectic)

c) $V^* = 3.62$

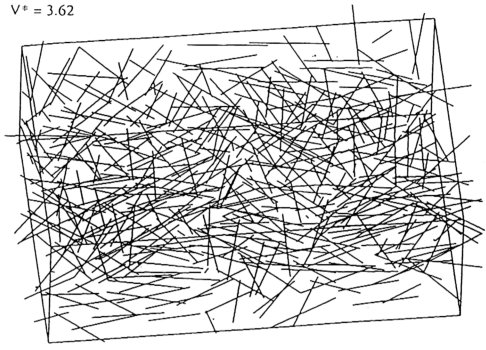

d) $V^* = 3.04$

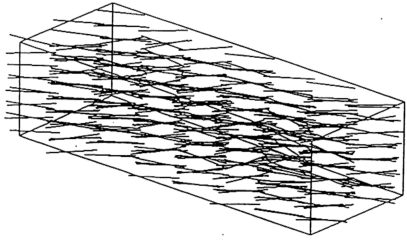

of the molecular orientations. The distribution of the centre of mass is also random confirming an **isotropic** phase. At next temperature which is at T* of 0.65, see Fig. 3.3 (b) the molecular centre of mass are still quite random, in accord with the identification, this is an **isotropic** phase. The box becoming elongated in shape while the volume decreases as the temperature decreases. The orientational order increase significantly on lowering the scaled temperature to T* of 0.55, as is apparent from the configuration shown in Fig. 3.3 (c). The order parameter, P_2 has increase drastically from 0.28 at T* of 0.60 to 0.94 at T* of 0.55. In Fig. 3.3 (d), the molecular organisation with respect to the director is more highly ordered where the director was found to remain more or less along the body diagonal of the simulation box. The layer structure, an important feature in **smectic** phase, is clearly appear in Fig. 3.3 (d) for T* of 0.55. Considerable enhancement of the translation order is also obvious with nine smectic layer which are manifestly apparently.

There are three possible types of these smectic phases, whether it could be as **smectic hexatic B (Hex B)** , **smectic crystal B (Cr B)** or **smectic A** ; therefore further investigation will carried out where the molecular organisation within the layers are examine in details. In order to visualize the distribution of the molecules within a layer, the image at T* of 0.55 was rotated into a frame of reference where the director aligned along one of the box's dimension. The rotated box are now consists of three layers formed a new configuration which was allowed to equilibrate by performing a further simulation run (see Fig. 3.4 (a)). The result is given in Fig. 3.4(b), where the centre of mass represented as "x" and these are found to be distributed randomly within the layer.

a)

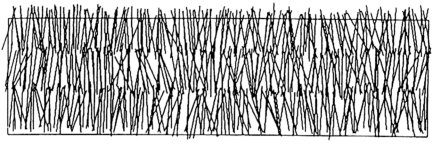

b)

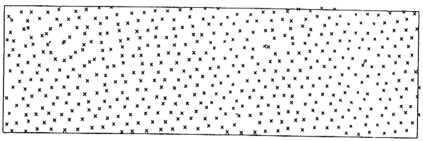

Fig. 3.4 Results of smectic phase at T^* of 0.55 :

a) The rotated box was allowed to equilibrate and the three layers are visible.

b) The projection of center of mass label "x" from the rotated box, results in some apparent vacancies.

When the simulated box is viewed from top, where all the layers are superimposed, the centre of mass (COM) distribution does not show perfect arrangement expected of a perfect crystal or that of a smectic CrB structure (where there should exist ABABAB packing correlation); instead there exist some obvious vacancies (see Fig. 3.4(b)) which strongly suggest lack of correlation between layers. The possiblities of having CrB for this phase is ruled out since there seems to be no interlayer correlation. Further investigate is performed where each of the three layers are examined separately; and the distribution of mass are represented as "1", "2", "3" for each layer respectively (see Fig. 3.5). It is obvious that the distribution of the centre of mass (COM) within the plane form a perfect hexagonal net. With a limited results and for such a small system it is very difficult to decide on the precise character of the transitional order and bond orientational order within the smectic plane. However, the tendency of the centres of mass to form a hexagonal arrangement suggest strongly that this phase is a mesogenic **smectic B (SmB),** unlike smectic A the centre of mass are found to be distributed randomly within the layer (for top view) [70]; as a results, smectic A is also rule out. Moreover the existence of long range bond orientational order in addition to the absence of long range positional order is the main feature of hexatic phase [78,79].

The artefacts

Irregularities have been observed previously for the smectic B phase form by the Gay-Berne mesogen [68,70,80]. In all these simulation, molecular dynamic technique was employed and volume of the system was held constant. However, the use of a

Side view

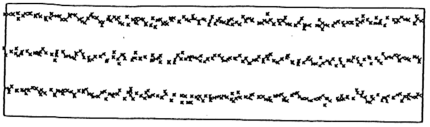

Top view of each layer.

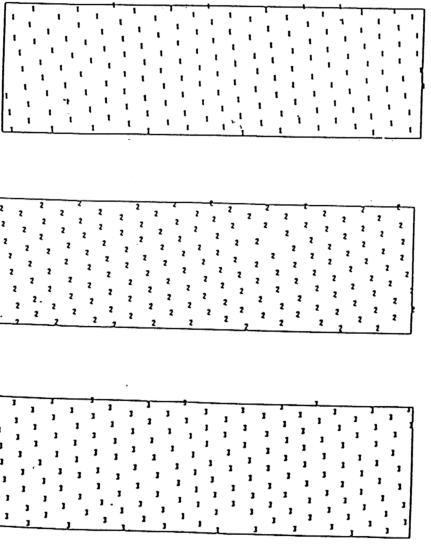

Fig. 3.5 Snapshot at $T^* = 0.55$, $P^* = 1.0$ showing the inplane positions of the molecular centres of mass of each layer denoted by the simbol itself. These layers represent a smectic B phase.

constant volume constraint may well create some iiregularities. One of these iiregularities include that the layer normal always appears to be aligned along the body diagonal of the simulated box [70]. In addition, the layer thickness of the smectic B phase was found to be about $2.6\sigma_0$ much shorter than the molecular length which was $3.0\sigma_0$ as specified by the parameter ($\sigma_{ee}/\sigma_{ss} = 3$), which implies a high degree of interdigitation [80]. Some of these artefacts explained above were also observed in our simulation (where the pressure was held constant) as indicated in Fig. 3.6. Apart from that, the tilted smectic B phase was also observed [68]. Fig. 3.7(a) shows the smectic layers are tilted to some extent with respect to the direction parallel to the layers. The equilibrated box in Fig. 3.6 was rotated into the director frame where the director axis is along the z- direction as shown in Fig. 3.7(a). The rotated box were again equilibrated and as a result, the tilted structure diminished (see Fig. 3.7 (b)). This occurs because in the constant pressure condition, the dimension of the orthogonal simulation box were allowed to vary independently thus reveal the true structure.

3.3.2 Thermodynamic Results

The thermodynamic properties evaluated during the production stage of the Monte -Carlo simulations were the scaled internal energy per particle, U*, the scaled volume per particles, V*, and from these the scaled entalpy per particle H*, where

$$H^* = (U^* + p^* V^*) \qquad (3.18)$$

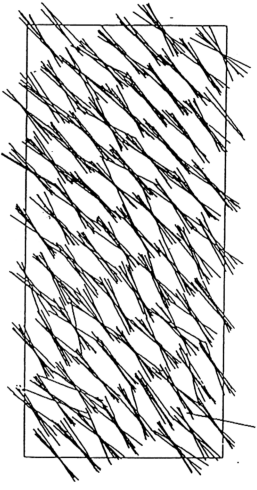

Fig. 3.6 Results of $T^* = 0.55$, on cooling simulations shows that the molecules are highly interdigitated. The director are along the body diagonal of the simulated box.

a)

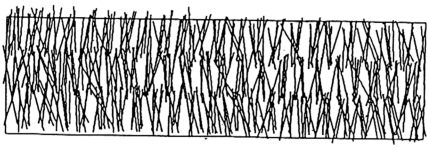

Side view

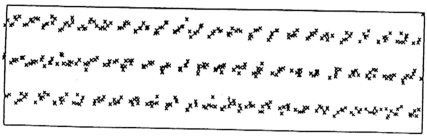

Centres of mass side projection view

Fig. 3.7 a) Before equilibration, the smectic layers are significantly tilted compare to b) after equilibration, the tilted effect are vanished but the ripple are sightly observed.

b)

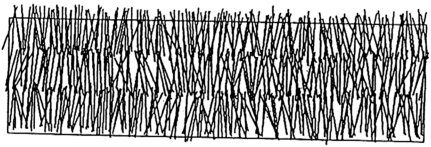

Side view

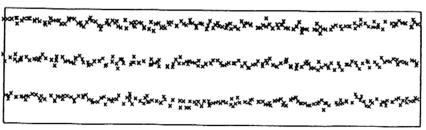

Centres of mass side projection view

The orientational order was monitored via the second- rank order parameter, P_2,

$$\overline{P_2} = \frac{3}{2}\langle \cos^2 Q_{ij} \rangle - \frac{1}{2} \qquad (3.19)$$

where Q_{ij} is the angle between the director and the molecular symmetry axis. The heat capacity, C_ρ*,was obtained from fluctuation of the energy, and via the direct differentiation of $\delta H / \delta T$ and other properties such as the density, ρ, was also calculated.

Histeresis

The thermodynamic results of cooling and heating cycles for both sets of simulations are shown in Table 3.1. Different thermodynamic properties are plotted against the reduced temperature namely graph 3.1, 3.2, 3.3, 3.4, 3.5 for a system of 500 particles. In these graphs, there exist discrepancies between the results for the cooling and heating cycles. The discrepancies lie at reduced temperature, T* between 0.55 to 0.60 only, whereas other temperature the results from both the cooling and the heating cycle agrees with each other.

In the cooling cycle, the system exhibit an isotropic phase at reduced temperature of 0.60 and above which is (T* = 0.80, 0.70 and 0.65) whereas in the heating cycle at (T* = 0.60, 0.55, 0.50, 0.45 and 0.40) corresponded to the smectic phase. In order to eliminate any uncertainty, the simulation was repeated and the equilibration period takes about 10 millions cycles of MC steps which is equivalent to 21 days in CPU time on RISC 350/6000 terminal. Extremely long equilibration runs

Table 3.1 (a) A summary of the results obtained from the cooling cycle of MC simulations.

T*	U*	error	H*	error	dH*/dT*	Cp*	error	V*	error	rho	P2bar	error
0.4	-5.84	4.00E-03	-2.95	4.00E-03	4.4	4.71	0.21	2.89	1.00E-03	0.35	0.96	3.00E-04
0.45	-5.67	0.01	-2.73	0.01	4.1	4.69	0.42	2.93	1.00E-03	0.34	0.96	9.00E-04
0.5	-5.52	0.01	-2.54	0.01	4.89	4.72	0.4	2.98	1.00E-03	0.34	0.95	6.00E-04
0.55	-5.27	0.01	-2.24	0.01	28.29	5.64	0.44	3.04	1.00E-03	0.33	0.94	7.00E-04
0.6	-3.33	0.01	0.29	0.01	28.3	5.45	0.64	3.62	3.00E-03	0.28	0.03	0.01
0.65	-3.13	0.01	0.59	0.01	5.3	4.75	0.72	3.73	4.00E-03	0.27	0.07	0.01
0.7	-2.99	0.01	0.82	0.01	4.67	4.91	0.82	3.82	0.01	0.26	0.04	0.01
0.75												
0.8	-2.73	0.01	1.29	0.02	4.7	4.1	0.2	4.02	0.006	0.25	0.01	-0.01

Table 3.1 (b) A sumarry of the results obtained from the heating cycle of the MC simulations previously.

T*	U*	error	H*		dH*/dT*	Cp*	error	V*	error	rho	P2bar	error
0.4	-5.64	0.01	-2.71	0.01	3.77	4.2	0.3	2.94	4.00E-03	0.34	0.96	1.00E-03
0.45												
0.5	-5.34	0.01	-2.33	0.01	3.98	6.4	1.8	3.01	4.00E-03	0.33	0.94	2.00E-03
0.55	-5.17	0.01	-2.11	0.01	5.2	4.7	0.8	3.06	4.00E-03	0.33	0.93	2.00E-03
0.6	-4.94	0.02	-1.81	0.02	27.1	7.2	1.6	3.12	4.00E-03	0.32	0.92	2.00E-03
0.65	-3.13	0.01	0.6	0.01	26.4	4.4	0.8	3.73	0.01	0.27	0.06	2.00E-02
0.7	-2.98	0.01	0.83	0.02	4.8	4.5	0.5	3.82	0.01	0.26	0.05	0.01
0.75	-2.84	0.01	1.08	0.02	4.6	3.3	0.3	3.92	0.01	0.26	0.04	0.01
0.8	-2.73	0.01	1.29	0.02	4.2	4.1	0.2	4.02	0.01	0.25	0.01	0.02

Table 3.1 Comparison of results from cooling and heating cycles for the isotropic and smectic phase of the Gay-Berne mesogen.

were conducted especially close to the smectic-isotropic phase transition where the behaviour of the system become sluggish, to create smectic B order from the isotropic phase. Consequently there is a possibility of histeresis observed at the smectic B-isotropic transition; i.e particularly when the system follows a different path especially the cooling cycle started off from the isotropic to form the smectic phase whereas the heating cycle started off from the smectic phase instead.

In order to understand the behaviour of the system at molecular level, the molecular organisation was further characterised with the aid of computer graphic at smectic-isotropic transition period. Snapshot of particles configuration has been taken at regular interval over a total of 10 million of Monte-Carlo steps. In this movie we observed the system starting from a disordered state, gradually increases it order but as the order parameter reached about 0.3, the order gets destroyed and this pattern was repeated several time over the total of Monte-Carlo steps. The behaviour can be explain through an anology as follows. Consider the sketched in Fig. 3.8, we can imagine that the system finds itself in region A of the configuration space, while we would like it to reach region B. This is not impossible, since there exists an open path from A to B , but the process may require a very long time due to the bottleneck shape of the pathway. Generally a non- equilibrium state like A having a relatively long lifetime is sometimes called a "metastable state" or "quasi-erogodic" behaviour (see appendix 3.2). At the smectic - isotropic transition phase the system is experiencing a " quasi erogodic behaviour" where in the regions of phase space which act as barriers and could cause bottlenecks. When a particles has a parallel arrangement as shown in Fig. 3.9 may prove

Fig. 3.8 Two hypothetical region of configurational space joined by a bottleneck pathway.

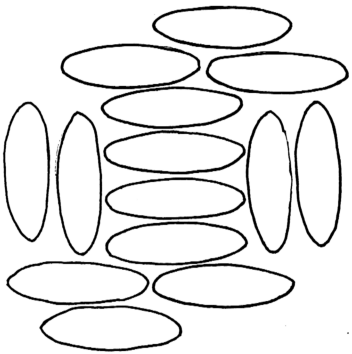

Fig. 3.9 A relatively stable configuration for a system of elongated particles.

difficult to unlock. This problem which is associated with histeresis have been reported every now and then particularly important in simulations of liquid crystals formed of hard elongated particles such as spherocylinder and ellipsoid of revolutions [68,70,81,82,83,84]. As for the Gay-Berne particles is considered as "soft potential" but also has a "hidden hard" of the ellipsoidal " shape" and thus is is not surprising that histeresis behaviour is observed. In future works, the T^*_{SI} transition period need to be explore at smaller range of reduced temperature interval say within 0.2. We have clarified the phenomena at transitional temperature, from now onwards we shall only concentrate analysing results of the Monte - Carlo simulation, begining with the scaled internal energy and enthalpy per particle.

Scaled Internal energy and Enthalpy per particle

The scaled internal energy, is shown as a function of temperature in Graph 3.1. This is negative as expected for a system at moderate pressures and exhibit a jump at the phase transition. The scaled enthalpy calculated from the internal energy and volume (see equation 3.18) is also given in Graph 3.2. The P*V* term makes a significant contribution to the enthalpy so much so that in the isotropic phase H* becomes positive. The enthalpy change across the transition was found to be 2.0, by extrapolating the results for H* in both phases back to the phase transition at T* of 0.575. This is so much higher than that for a system of nematic liquid crystal with pairwise interaction, where the change in the scaled enthalpy across the transition is only 0.6 [85]. These observation are due to be expected because the former involves a transition from an

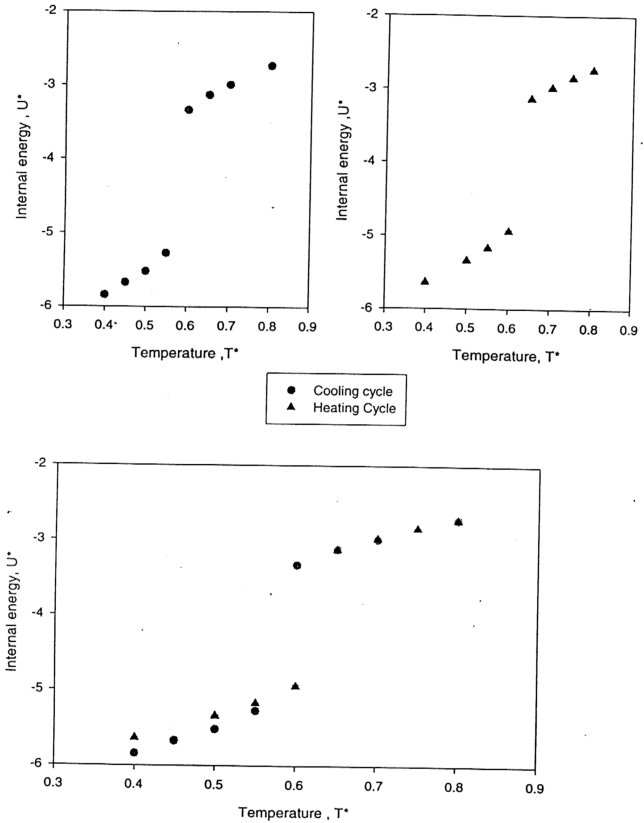

Graph 3.1 Dependence of the scaled internal energy, U*, on the scaled temperature, T* for the isotropic and smectic B phase of the Gay-Berne mesogen.

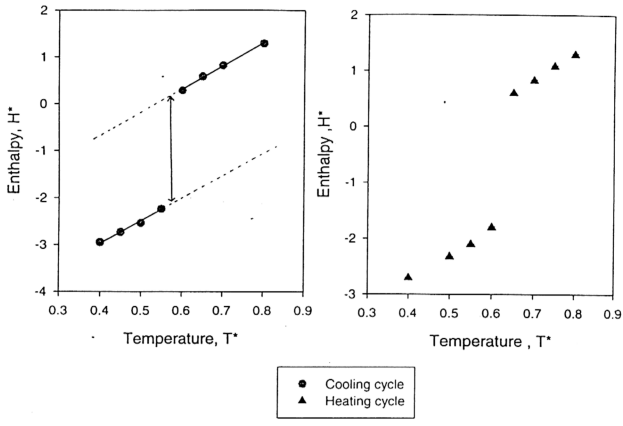

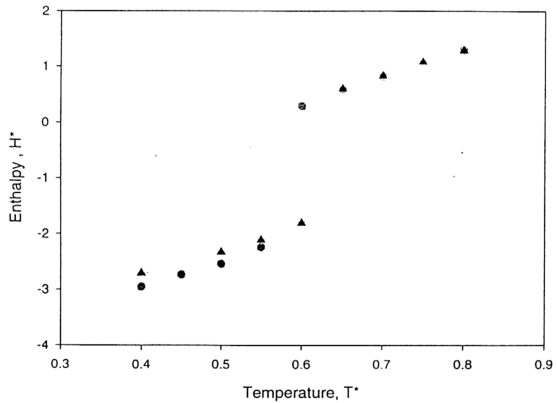

Graph 3.2 Dependence of the scaled enthalpy, H*, on the scaled temperature, T*, for the isotropic and smectic B phase of the Gay-Berne mesogen.

isotropic phase to a more ordered phase (smectic B) while the latter is a transition from nematic to isotropic phase. Strong transitional features can also be seen in other properties like the scaled volume per particle.

Volume per particle

The volume per particle, V*, which is shown as a function of reduced temperature, T* are plotted in Graph 3.3. From the graph the volume has steadily decrease from T* of 0.55 to 0.40. This is due molecular organisation in the smectic phase which packed close to each other. In the isotropic phase ranging T* of 0.6 to 0.8, where molecule are distributed more randomly arranged, the box dimension expanded significantly to a value of 4.0.

There is a clear jump in the volume between T* of 0.55 and 0.60 indicating the strong first-order nature expected for an isotropic- smectic B transition. By assuming a linear dependence of V* , the volume transition ΔV^* was estimated to be 0.50 ± 0.01. The transition temperature T^*_{SmB-I} is 0.575 was located midway between the highest temperature in the smectic B phase and the lowest in the isotropic region. The uncertainty in this value is half the difference between these two temperatures, namely ± 0.025. However, the uncertainty may be larger because of the possibility of hysteresis at the isotropic-smectic B transition; we have not explored possibility in any detail since extremely long equilibration runs are needed to create smectic B order from the isotropic phase.

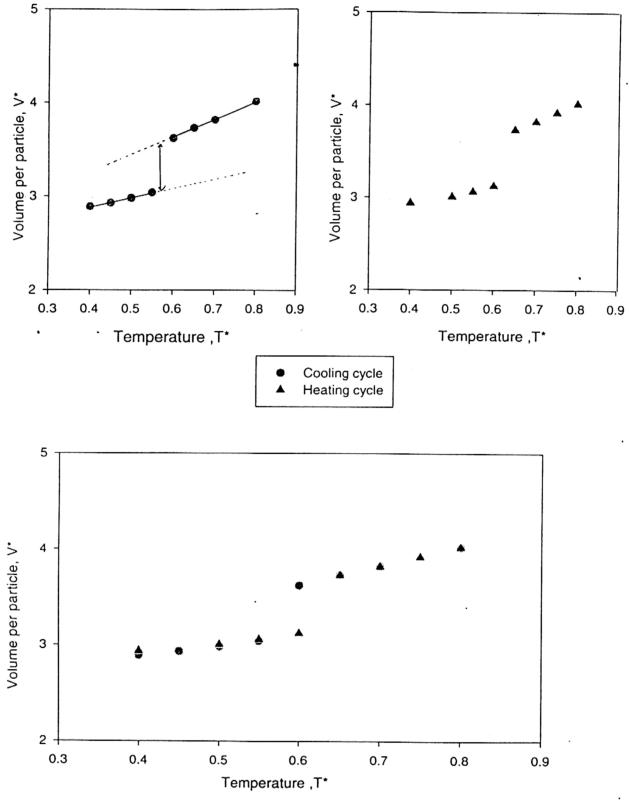

Graph 3.3 The scaled Volume per particle against scaled Temperature determine at constant pressure.

Heat Capacity

The variation of reduced heat capacity calculated with temperature shown in Graph 3.4. Divergence is observed in the curve between $T^* = 0.55$ and $T^* = 0.60$ suggesting the occurrence of the isotropic -smectic transition. This give a transition point of $T^*_{I\text{-}SmB} = 0.575 \pm 0.0025$ which was also supported by other thermodynamic properties plotted in previous section. From the graph plotted, it was also found that $Cp^*$is less than 30, while that for alkane hydrocarbons the value is typically about 20.

Second rank order parameter

We finish this section by describing our results for the second -rank orientational order parameter,$\overline{P}_2$. It is the only orientational property calculated directly in the simulation; this is shown as a function of the scaled temperature in Graph 3.5. The system is isotropic at a reduced temperature of $T^*= 0.80$ and remains orientationally disordered until the temperature is lowered to about 0.55. In the range of reduced temperature from 0.55 to 0.40, the order parameter is near to one which is the smectic phase. As for the isotropic phase , the order parameter is less than 0.02 but not quite zero. This is due to the finite size of the system which consist only 500 particles [86] (describe earlier in chapter 2). There is then a large jump in $\overline{P}_2$ to a value of ca. 0.85 of $T^* = 0.575$, which again consistent to the observation of a strong first-order transition as previously discovered. The orientational order for a system which undergoing the smectic-isotropic transition has been studied indirectly by using an aminoxyl spin probe with similar dimensions to the smectic host is the ethyl 4- azoxybenzoate [87]. Here the

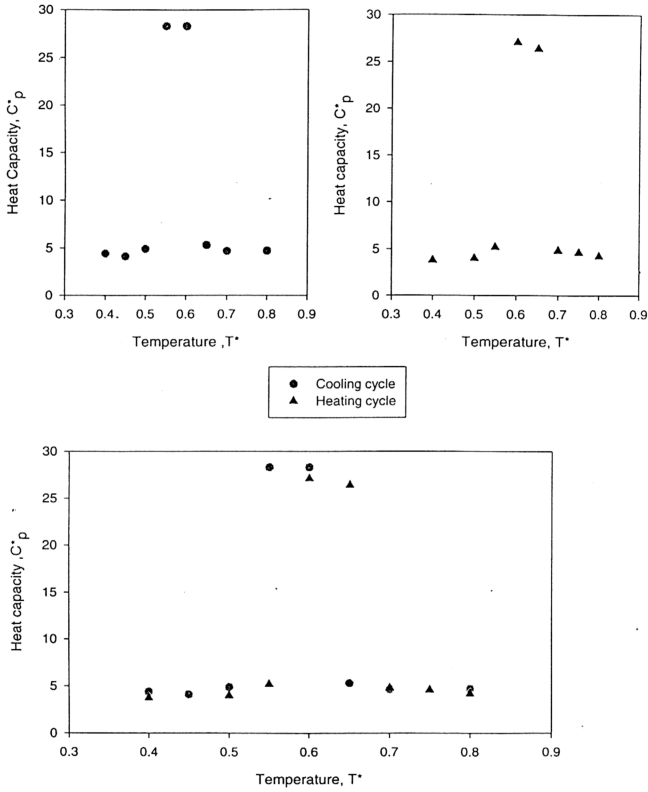

Graph 3.4 Variation of scaled heat capacity, C^*_p , with the scaled temperature, T* showing a strong jump at I-S transition

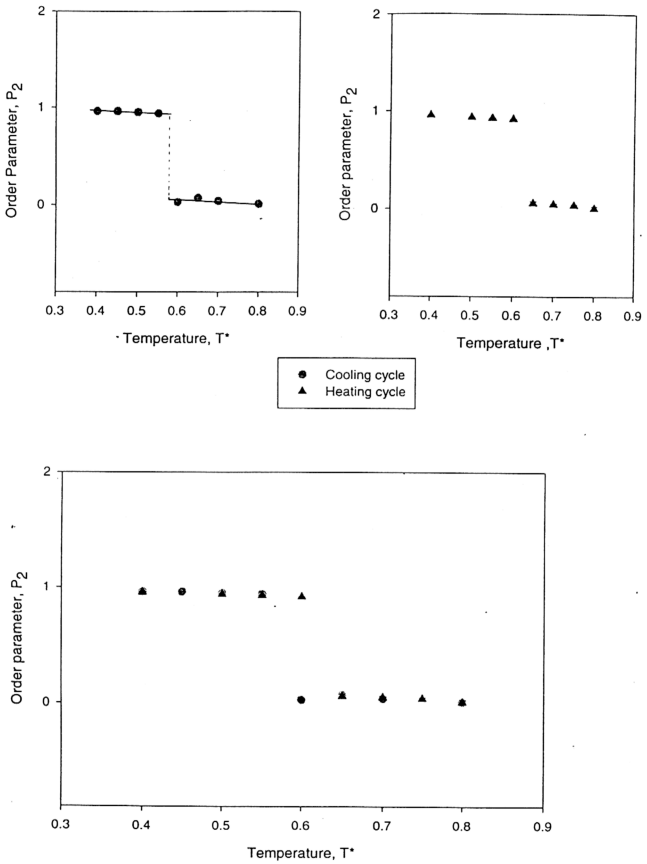

Graph 3.5 Variation of the second-rank orientational order paramater, P_2 with the scaled temperature,T*, for the Gay-Berne mesogen.

second -rank order of the aminoxyl guest was found to be 0.88 which is in good accord with the simulation.

3.4 Cooling "time"

Computer simulations of the structure and dynamics of material concentrated mainly on either on the micrroscopic evolution of a system, typically less than a few nanoseconds (1 ns = 10^{-9}s) in duration, or the equilibrium structure and properties of the system in the steady state. For instance, molecular dynamic (MD) computer simulations are often used to determine the microscopic motions of a system as a function of time and predict the associated microscopic mechanisms. Due to avery small time steps in femtosecond (~ 10 -^{15} s) and the simulation cell size constrainted to about (~ (100 Å)^3), MD simulations cannot describe the macroscopic properties of the system that evolve over longer periods of time and larger domains size. On the other hand techniques such as Monte-Carlo (MC) simulations predict steady state properties and structures at the expense of the microscopic details of time- dependent dynamics. There has been recent attempts to bridge the chasm between the two approaches by way of kinetics [88-92] and the time dependent Monte -Carlo methods[93-99]. These new MC methods include the retention of the microscopic dynamics through the rates and probabilities of predetermined microscopic processes and yet overcome the time and size constraints typical of the MD methods. Consequently these MC methods allow access to both the microscopic regime of MD simulations and the macroscopic regime of conventional MC

simulations. There have been significant developments as these MC methods have evolved toward the realistic simulation of dynamic systems. The definition of the MC time step and its relationship to real experimental time has been rigorously sought [93-99]. As an example the time-dependent Monte- Carlo (TDMC) method [100], has been used to predict the density and distribution of C radicals on the diamond{001} (2x 1): H surface under hot filament, chemical vapor deposition (CVD) growth conditions. The simulation time step is the real time step in which all particles are allowed to move simultaneously, albeit probabilistically.

In this thesis, a simple alternative approach which relate the simulated time to the real time is presented. Focus will be on the dynamical interpretation time steps of simple Monte Carlo method by means of calculation. The system studied consists of 500 particles of NpT ensemble interacting via Gay -Berne potential. These system was cooled from reduced temperature of 0.80 which is in isotropic phase to a reduced temperature of 0.40 which exhibited the smectic B phase. The aim of this study is to determine the duration of the time involved in the cooling process. Calculation were carried out using both time-steps from the MC simulated results and that of the MD[101,102]. These time -steps results were also compared with other simulated system's time steps like benzena, water, carbon disulphite and etc.

Derivation of time-steps, δt

In order to derive the MC time steps, a few assumption has to be made. Firstly the equation of average displacement for a particle can be taken as a half maximum of

displacement as below,

$$\delta r_{avg} = \frac{1}{2}\delta r_{\max} \qquad (3.20)$$

where δr is the displacement of a particle [103]. For a system composed of more than one particle, the average speed of particle i, is given as , v_i where

$$v_i = \frac{\delta r_{avg}}{\delta t} = \frac{\delta r_{\max}}{2\delta t}, \qquad (3.21)$$

and δt is the time steps. From the equipartitional theorem (appendix 3.2), the kinetic energy is equal , eq.(3.22)

$$\frac{1}{2}\sum_{i}^{N} m v_i^2 = \frac{3}{2} N_A k_b T, \qquad (3.22)$$

where N_A is the number of particles, k_b is the Boltzmann factor , T is a temperature in kelvin and a particle with a mass m. For only speed of i particle, where

$$v_i = \sqrt{\frac{3 k_b T}{m}}, \qquad (3.23)$$

substitution of eq. (3.23) into eq. (3.21) , the time step, δt becomes

$$\delta t = \frac{\delta r_{\max}}{2}\sqrt{\frac{m}{3k_b T}} \qquad (3.24)$$

Eq. (3.24) must be in the formed of reduced units. Substitution with formula of reduced temperature ,$T^* = k_b T$; the reduced maximum displacement as $\delta r^* = \sigma / r$ and the time steps formula, $\delta t = \delta t^* \sqrt{(m\sigma_0^2/\epsilon)}$, the reduced time step is shown as in eq. (3.25),

$$\delta t^* = \frac{\delta r^*_{\max}}{2\sqrt{3T^*}}, \qquad (3.25)$$

Finally the MC time steps, δt_{MC}

$$\delta t_{MC} = \frac{\delta r^*_{\max}}{2\sqrt{3T^*}}\sqrt{\frac{m\sigma_0^2}{\epsilon}}, \qquad (3.26)$$

where ϵ is the strength parameter, m is mass of a compound in kg per mol, σ_0 is the distance between nearest neighbour of a particle. In the simulation of generic Gay - Berne (GB) model like system, reduced units must be used because the counterparts of ϵ and σ are not assigned definitive values (see appendix 3.3).

Calculation of time steps

In order to calculate the time steps (refer to the eq.(3.26)), certain parameter such as δr^*, T^*, ϵ, σ and m need to be obtained first. The system used in this simulation adopted the Gay - Berne original parameterization scheme, namely, $\sigma_{ee} / \sigma_{ss} = 3$ and $\epsilon_{ss} / \epsilon_{ee} = 5$, $\nu = 1$, $\mu = 2$. An example of a typical molecules which match this size parameter were like 4,4 '-dimethoxyazoxybenzene (PAA), ethyl-4-azoxybenzoate (smectic host), 4-hexyloxy-4'-cynobiphenyl (smectic B), 4 -methoxybenzylidene -4' -n-butylaniline (MBBA) and etc. In this thesis however, 4,4 '-dimethoxyazoxybenzene (PAA)[55] has been selected as a model since this is a reasonably rigid molecule which length to breath ratio of 3 : 1. In addition, it has been well studied experimentally. The experimental data for the nematic-isotropic transition temperature, T_{NI} of PAA is 408K at atmospheric pressure (i.e. 1.01×10^5 N m^{-2}) which gives a value for ϵ of 1.88 kjmol^{-1} (equivalent to 3.12×10^{-21} J per particle) and the nearest-neighbour separation, σ_0 of 4.5×10^{-10} m. The mass per particle, m was calculated to be 2.358×10^{-25} kg.

In the smectic, phase the scaled pressure, p^* was set equal to one. This value was chosen because it is sufficiently low to stabilise the smectic B phase where the reduced temperature was found to be at 0.55. Using PAA data experimental value whereby ($\epsilon = 1.88$ kJmol^{-1}, $\sigma_0 = 4.5 \times 10^{-10}$ m, $m = 2.358 \times 10^{-25}$ kg) and also δr_{max} is the maximum displacement parameters, were obtained from an input in the simulation which calculated to be 0.0958. Substitution of these values in (eq. 3.26), the time steps, δt_{MC} in smectic phase were calculated to be 1.458×10^{-13}s.

Using the previous MD simulation results [101,102], δt_{MD} is calculated as .

follows. Assuming that the same molecule that we used , 4,4' -dimethoxyazoxybenzene whereby the data provided were T_{NI} is at 408K , pressure is at 1 atm , ϵ = 1.88 kjmol^{-1}, σ_0 is 4.5e-10m, the mass per particle estimated 2.358×10^{-25} kg and δt^*_{MD} = 0.005 [101,102]. Calculation were performed using the equation of time steps ($\delta t = \delta t^* \sqrt{(m\sigma_0^2/\epsilon)}$), δt_{MD} was found to be 1.955×10^{-14}s. In order to test the reliability of the time step results, a comparison with a reported experiment findings and our results were tabulated in Table 3.2.

From the Table 3.2(a), the δt_{MC}, obtained for PAA using the nematic-isotropic transition properties, was found to be in broad agreement in the order of magnitude with that of δt_{MD} calculation of PAA Table 3.2 (a). However the δt_{MC} calculated for p^* =1, using the same PAA transitional (to obtain ϵ, σ) data gave a value much bigger by a factor of 10. This discrepancy could well be due to the fact that the transitional data of nematic - isotropic was used and extrapolated while the δt_{MC}^* in this case is obtained for isotropic-smectic transition. The magnitude of these time steps were comparable to those of other systems (see Table 3.2 (b)) especially the site-site atomic interaction of planar C_6H_6 [105] since both system (4,4'-dimethoxyazoxybenzene (PAA) and C_6H_6 has had a ring system. Others system like the rigid linear triatomic fluid e.g. CS_2 [106], rigid triatomic molecule like H_2O [107], linear N_2 [108] and also the rigid polyatomic molecule such as CH_4 [109] were also compared.

Finally, to obtained the real time for the cooling process of isotropic-smectic transition the time steps of smectic phase, δt_{MC} were converted into real time by multiplying with the total number of MC steps, (i.e.20×10^5 MC steps) which gives a

Table 3.2 (a)

Phases	Technique	System	p^*	δr^*	T^*	ε / kJmol^{-1}	δt / s
Smectic	MC	PAA	1.0	0.09578	0.55	1.88	1.376×10^{-13}
Nematic	MD	PAA	-	-	-	1.88	1.955×10^{-14}

Table 3.2 (b)

References	Technique	System	δt / s
Rahman and Stillinger	MD	H_2O	4.355×10^{-16}
Tidesley and Madden	MD	CS_2	4.480×10^{-15}
Cheung and Powles	MD	N_2	6.000×10^{-15}
Ciccotte et al	MD	CH_4	2.400×10^{-15}
Evans and Watts	MD	C_6H_6	$\sim 1 \times 10^{-14}$

Table 3.2 Comparison results of time steps, δt from a) using the PAA and b) previously studied systems.

appoximated value of 2.916×10^{-7} s or ~ 0.3 microsecond. This values indicate that cooling process takes place within microsecond range which is short but not unrealistic. Such is a very typical advantage of a computer "experiment" which allowed us to detect event that takes place within microsecond (10^{-6}) time limit whereas observing such event in the laboratory were practically difficult. The real time steps for MC was obtained by converting the "simulated time-step" by extrapolating certain data and introducing various approximation. This approach may be controversial but nevertheless it is a first attempt to estimate the " cooling time". Perhaps in the future there would be a better way of obtaining the real MC time.

3.5 Conclusions and Future Works

The constant-pressure Monte-Carlo simulations have been undertaken to investigate the thermodynamic properties and structure of the cooling cycles of the Gay-Berne mesogens. The use of isothermal- isobaric condition facilitates comparison with experiment and it is found that the volume change are typical of those expected for a isotropic-smectic B transition. The second-rank orientational is found to be ca. 0.85 at the transition, again in agreement with experiment. There is histeresis expected at the isotropic- smectic transition whereby the thermodynmic results show a discrepancies at the reduced temperature of 0.55 to 0.60. This suggest that the system is experiencing a quasi erogodic behaviour due to different path taken. It would be clearly be interest to study the transition again within smaller range, but this was not undertaken in our

simulation, perhaps in near future.

The phase is determine visualisation of the molecular organisation in a single configuration where the hexagonal structure of the phase and short range correlation between the positions of particles in different layers, confirm as smectic hexatic B phase. Some irregularities are observed such as the director are always found to be align at the body diagonal of the simulation box and interdigitation of particles in the adjacent layers. In constant-pressure simulation, with the ability of the size of the simulation box to change, it is likely that this irregularities is a natural feature of the phase. As for the tilted structure of smectic-B phase, after a long equlibration runs the tilted has vanished. This confirm that it is not an artefact of the periodic boundary condition instead it is due to NpT simulation which relax the simulation box.

An approach to measure the MC time -step, δt_{MC} are introduced. This method are discussed and results are in broad agreement with previous studies. In addition the cooling time of the formation smectic B phase is found to be in the region of microsecond!. In future undertaking, this approach could be well studied in details with better improvement.